Nationaal Lucht- en Ruimtevaartlaboratorium
National Aerospace Laboratory NLR

NLR-TP-97268

On thermal-gravitational modelling, scaling and flow pattern mapping issues of two-phase heat transport systems

A.A.M. Delil

Nationaal Lucht- en Ruimtevaartlaboratorium

National Aerospace Laboratory NLR

NLR-TP-98268

On thermal-gravitational modelling, scaling and flow pattern mapping issues of two-phase heat transport systems

A.A.M. Delil

Updated part of NLR-TP-98170, prepared for presentation (as SAE 981692) at the 28th International Conference on Environmental Systems, July 13-16, 1998, Danvers, MA, USA.

Division:	Space
Issued:	June 1998
Classification of title:	Unclassified

Cont ents

1 Table
10 Figures

(14 pages in total)

981692

On Thermal-Gravitational Modelling, Scaling and Flow Pattern Mapping Issues of Two-Phase Heat Transport Systems

A.A.M. Delil
National Aerospace Laboratory NLR, Space Division
P.O. Box 153, 8300 AD Emmeloord, Netherlands

ABSTRACT

The paper deals with heat and mass transfer research issues related to the development of spacecraft active thermal control systems, more specifically development of two-phase heat transport system technology. It focuses on design and development supporting theoretical work: the thermal/ gravitational scaling of two-phase heat transport systems, including the aspects of gravity level dependent two-phase flow pattern mapping and condensation.

INTRODUCTION

Thermal management systems for future large spacecraft have to transport large amounts of dissipated power (up to 200 kW) over large distances (up to 100 metres). Conventional single-phase heat transport systems (based on the heat capacity of the working fluid) are simple, well understood, easy to test, relatively inexpensive and low risk. But to realise a proper thermal control task with small temperature drops from equipment to radiator (to limit radiator size and mass), they require thick walled, large diameter, heavy lines and noisy, heavy, high power pumps, and therefore large solar arrays.

As an alternative for these single-phase systems one considers mechanically pumped two-phase systems: being pumped loops which accept heat by evaporation of the working fluid at heat dissipating stations (cold plates, heat exchangers) and release heat by condensation at heat demanding stations (hot plates, heat exchangers) and at radiators, for rejection into space. Such a system relies on heat of vaporisation: it operates nearly isothermally and the pumping power is reduced by orders of magnitude, minimising radiator and solar array sizes. Ammonia is the most promising candidate working fluid.
The stations can be arranged in a pure series, a pure parallel or a hybrid configuration. The series configuration is the simplest, it offers the possibility of heat load sharing between the different stations, with some restrictions with respect to their sequence in the loop. However, the series configuration has very limited growth potential and the higher flow resistance.

In the low resistance modular parallel concept (e.g. ESA´s Two-Phase Heat Transport System, TPHTS), the stations operate relatively independently, thus offering full growth capability. However, the parallel configuration is more complicated, especially when redundancy and heat load sharing (some cold plates operating in reverse mode) is foreseen. In addition, a parallel configuration requires a control system consisting of various sensors, monitoring the loop performance at different locations, control logic and actuators to adjust e.g. pump speed, fluid reservoir content and throughputs of valves. Sensors necessary for control are pressure gauges, flow meters, temperature gauges and vapour quality sensors (VQS), measuring the relative vapour mass content of the flowing mixture. An important application for VQS is at the cold plate exits, as a part of a control (sub-)system, adjusting the liquid fed into the cold plate to prevent the dry-out of the evaporator, or maintaining a prescribed quality value at evaporator exits, independent from transient heat sources and heat sink conditions (Delil, 1988, 1997, 1998).

An alternative for a mechanically pumped system is the capillary pumped system, using surface tension induced pumping action of capillary-type evaporators. Such capillary two-phase systems can be applied for instance in spacecraft not allowing vibrations induced by mechanical pumping (e.g. Dunbar, 1996). Ammonia is the most promising candidate working fluid for capillary-pumped two-phase thermal control loops also.

Two different systems can be distinguished (Cullimore & Nikitkin, 1998): the western-heritage Capillary Pumped Loop, CPL (Stenger, 1966; Cullimore, 1993), and the Russian-heritage Loop Heat Pipe, LHP (Bienert & Wolf, 1995; Maidanik et al., 1991 &1995).
Although initially perceived by many as alternatives to heat pipes at high transport powers (500W to 24kW), in recent years the intrinsic advantages of a small-diameter piping system without distributed wick structures have been exploited at low powers (20 to 100W). Many advantages of CPL and LHP are only truly exploited when these devices are considered early in the design, rather than treated as replacements for existing heat pipe based designs.

Advantages of CPL and LHP are:

The tolerance of large adverse tilts (meaning a heat source up to 4 m above a heat sink, facilitating ground testing and even enabling many terrestrial applications).

Tolerance of complicated layouts & tortuous transport paths.

Easy accommodation of flexible sections, make/break joints, and vibration isolation.

Fast and strong diode action.

Straightforward application in either fixed conductance or variable conductance modes.

Separation of heat acquisition and rejection components for independent optimisation of heat transfer footprints and even integral independent bonding of such components in larger structures.

Accommodation of mechanical pumps.

Tolerance of large amounts of noncondensible gases which means extended lifetime.

Because of their performance advantages, unique operational characteristics, and recent successful flight experiments, CPL and LHP technologies are currently gaining acceptance in the aerospace community. They are baselined for several missions including NASA's EOS-AM, JPL's MSP ("Mars '98"), ESA's ATLID, CNES's STENTOR, RKA's OBZOR and MARS 96 mission (a retrofit mission for the Hubble space telescope), COMET, the Hughes 702 satellites, and various other commercial geosynchronous communication satellites.

As two-phase flow characteristics and heat transfer differ when subjected to a i-g or a low-gravity environment, the technology of such two-phase heat transport systems, and their components, has to be demonstrated in orbit. Therefore several in-orbit experiments were recently carried out: TPX I (Delil, 1995, 1997), CAPL 1&2 (Butler et al., 1996; Ku et al., 1995) LHPFX (Baker et al., 1998), ALPHA and TPF (Ottenstein & Nienberg, 1998; Antoniuk & Nienberg, 1998). Others are planned for near-future spaceflights: TPX II (Delil et al., 1997), CAPL 3 (Ku et al., 1998; Kim et al, 1997), STENTOR (Amadieu et al., 1997), CCLP (Hagood, 1998), TEEM (Miller-Hurlbert, 1997), and Granat (Orlov et al., 1997).

DESIGN SUPPORTING THEORETICAL WORK

Supporting theoretical work, like the modelling and scaling of two-phase heat transport systems (Delil, 1991), is done:

- For a better understanding of two-phase flow and heat transfer phenomena.
- To provide means to compare and generalise data.
- To develop a useful tool for the design of two-phase flow systems and system components, in order to save money and to reduce costs.

Examples of the scaling of two-phase flow and heat transfer can be found in the power and in the process industry. The scaling of the physical dimensions is of major interest in the process industry: large scale industrial systems are studied using reduced scale laboratory systems. Scaling of the working fluid is of principal interest in the power industry: large industrial systems, characterised by high heat fluxes, temperatures, and pressures, are translated in full size systems operating at more attractive lower temperature, heat flux and pressure levels (scaling a high pressure water-steam system by a low pressure refrigerant system of the same geometry).

The main objective of scaling space-oriented two-phase heat transport systems and system components is the development of reliable spacecraft systems, of which the proper reduced gravity performance can be predicted using results of experiments with scale models on earth.

Scaling spacecraft systems can be useful also:

- For in-orbit technology demonstration, e.g. the performance of spacecraft heat transport systems can be predicted based on the outcomes of in-orbit experiments on model systems with reduced geometry or different working fluid.
- To define in-orbit experiments intended to isolate typical phenomena to be investigated, e.g. the excluding of gravity-induced disturbing buoyancy effects on alloy melting, diffusion and crystal growth, for a better understanding of the physical phenomena.

The magnitude of the gravitational scaling varies with the objectives:

- From 1 g to 10^{-6} g (random direction) for the terrestrial scaling of orbiting spacecraft.
- From 1 g to 0.16 g for Moon base and to 0.4 g for Mars base systems.
- From 10^{-2} or 10^{-6} g to 1 g for isolating gravity-induced disturbances on physical phenomena under investigation.
- From low g to another or the same low-g level for in orbit technology demonstration (e.g. in a Keplerian aircraft trajectory) or sounding rockets.

One-g is not the upper limit in gravitational scaling: higher values can be obtained during special aircraft trajectories, or by rotation e.g. the centrifugal scaling of isothermal separated gas-liquid flow in a tube, fast rotating a vertical tube around an external vertical axis (Geraets, 1986).

Unfortunately, even in single-phase systems scaling is an all except simple problem, since flow and heat transfer are equivalent in the model and the original (prototype) system only if the corresponding velocity, temperature and pressure fields are identical. Dimensionless numbers can be derived either from the conservation equations for mass, momentum and energy or from similarity considerations, based on dimension analysis. The aforementioned identity of velocity, temperature and pressure fields is obtained if all dimensionless numbers are identical in model and prototype.

Scaling two-phase systems is far more complicated because:

- In addition to the above fields, spatial density distribution (void fraction, flow pattern) must be considered.
- Geometrical scaling often makes no sense since some characteristic dimensions, e.g. bubble size and surface roughness, hardly depend on the system dimensions.
- Of the proportion problem, arising from high power density levels, typical for two-phase flow and (boiling) heat transfer.

SIMILARITY AND DIMENSION ANALYSIS - Similarity considerations, discussed in detail in Delil, 1991 & 1998, led to the identification of 18 dimensionless numbers (so-called B-numbers) which are relevant for thermal gravitational scaling of two-phase loops. These B-numbers are listed in Table 1.

As said before, perfect similitude between model and prototype is obtained if all dimensionless numbers are identical in prototype and model. There is perfect similitude and only then the scaling is perfect. It is evident that perfect scaling is not possible in the case of two-phase flow and heat transfer: the phenomena are too complex, the number of important parameters or B-numbers is too large.
Fortunately also imperfect (distorted) scaling can give useful results. Therefore a careful estimation of the relative magnitudes of the different effects is required. Effects that can be identified to be of minor importance make the identity of some B-numbers to a practically superfluous condition for the problem involved. Examples for a two-phase systems are: the Mach number is not of importance for the incompressible flow in the liquid lines, the Froude number (gravity) is not important in pure vapour flow.

Finally it is remarked that in scaling a two-phase heat transport system:
- Geometric distortion is not permitted to study boundary layer effects and boiling heat transfer, as identity of surface roughness in prototype and model is to be guaranteed.
- Geometrical distortion is a must when the length scaling leads to impractically small (capillary) conduits in the model, in which the flow phenomena basically differ from flow in the full size prototype.

Sometimes it is more convenient to replace the quality X by the volumetric vapour fraction (void fraction) α, according

$$(1-\alpha)/\alpha = S\,(\rho_v/\rho_l)/(1-X)/x. \qquad (1)$$

It is obvious that the set of B-numbers presented is a rather arbitrary one, e.g. several numbers contain only liquid properties. These can be easily transferred into vapour properties containing numbers using Π_6, Π_7 and Π_8. Similarly Π_1 can be used to interchange characteristic length (e.g. duct length, bend curvature radius) and a characteristic diameter (e.g. duct diameter, hydraulic diameter, but if desired also surface roughness or bubble diameter). Sometimes it will even be convenient to simultaneously consider two geometry Π_1-numbers: one for the overall channel (channel diameter versus length or bend curvature radius), the other pertaining to other parameters as the ratio of surface roughness and bubble diameter for investigating boiling heat transfer, or the ratio of surface roughness and channel diameter for studying frictional pressure drop.

The general approach in scaling is to choose combinations of n-numbers such that they optimally suit the problem under investigation.

Typical examples are:
- The Morton number

$$\Pi_{15} = Mo_l = Re_l^4 Fr_l/We_l^3 = \rho_l \sigma^3/\mu_l^4 g, \qquad (2)$$

which is especially useful for scaling two-phase flow with respect to gravity (since it contains, apart from gravity, only liquid properties and surface tension).
- The Mach number

$$\Pi_{16} = Ma = v/(\partial p/\partial \rho)^{1/2}, \qquad (3)$$

when compressibility effects are important (e.g. choking strongly depends on the vapour quality of a homogeneous two-phase mixture).
- The boiling number

$$\Pi_{14} = Bo = Q/\dot{m}\, h_{lv} = \Delta H/h_{lv} \qquad (4)$$

Q being the power fed to the boiling liquid. This number appears in the expression for the dimensionless enthalpy at any z in a line heated from outside

$$\Delta H(z)/h_{lv} = \Delta H_{sr}/h_{lv} + \pi D z q/\dot{m} h_{lv} \qquad (5)$$

q is the heat flux. For subcooled or heated liquid this becomes

$$\Pi_{14} = Q/\dot{m}\, Cp,\, \Delta T, \qquad (8)$$

ΔT being the pressure drop. The above implies that, if the dimensionless entrance enthalpies are equal for different fluids flowing in similar geometries, equality of the boiling number ensures equal dimensionless enthalpies at all similar axial locations. For thermodynamic equilibrium conditions' this means equal qualities at similar locations and similar subcooling and boiling lengths.
- The condensation number

$$\Pi_{17} = (h/k_l)(\mu_l^2/g\,\rho_l^2)^{1/3}, \qquad (7)$$

h being the local heat transfer coefficient.
- The vertical wall condensation number

$$\Pi_{18} = L^3 \rho_l^2\, g\, h_{lv}/\mu_l k_l (T_o - T_s). \qquad (8)$$

T_o is the local sink, T the local saturation temperature.

A first step in a practical approach to scale two-phase heat transport systems is the identification of the important physical phenomena, in order to obtain the n-numbers for which identity in prototype and model must be required to realise perfect scaling according to the so-called Buckingham's theorem (the crucial identity in similarity considerations). Distortion will be permitted for n-numbers pertaining to phenomena considered less important. That the important phenomena and the relevant B-numbers will be different in different parts of a system is obvious.

Table 1 shows the relevance (• means relevant) of the Π-numbers in the various loop sections.

For refrigerants like ammonia and R114, forced convection heat transfer overrules conduction completely. Therefore Π_{10}, Π_{11} and Π_{12}, are not critical in gravitational scaling. Π_{16} can be neglected also as the system maximum power level and line diameters correspond with flow velocities far below the sonic velocity in all parts of a system.
Considering Π_3/Π_5, it can be remarked that inertia overrules buoancy not only in pure vapour flow or in a low gravity environment, but also for horizontal liquid sections on earth ($\nu \rightarrow \pi/2$). This implies that there is n-number identity for these sections in low-g prototype and terrestrial model, for a horizontal arrangement of these sections. Also it can be remarked that, in the porous (liquid) part of a capillary evaporator, surface tension forces ($2\sigma/D_p$) are dominant over inertia ($\Pi_9 \rightarrow 0$). Consequently the evaporator exit quality will approach 1 (pure vapour). This means that gravity is unimportant for the vapour part of the evaporator and the vapour line connecting evaporator and condenser.

Important conclusions can be drawn now:
- The condensers and, in the mechanically pumped system also the two-phase lines, are crucial in scaling with respect to gravity. They determine the conditions for the evaporators and single-phase sections. The latter can be scaled in the classical way presented in text books.
- In the adiabatic two-phase lines (in the mechanically pumped mode) under low-gravity conditions only shear forces are expected to cause the separation of the phases in the high-quality (above say 0.8) mixture, leading to pure annular flow (a fast moving vapour in the core and a by frictional drag induced slowly moving liquid annulus at the inner line wall) for the lower flow rates. For increasing power, hence flow rate, the slip factor will increase introducing waves on liquid-vapour interface and entrainment of liquid droplets in the vapour: so-called wavy annular/ mist flow. A similar flow pattern behaviour can be predicted for vertical downward flow on earth, as it easily can be derived from the flow pattern map for downward two-phase flow (Fig. 1), taken from Oshinowo & Charles, 1974), in which water properties at 20 °C must be used to determine the scale of the abcissa.
  The Froude number for two-phase flow used in this figure is defined as:

$$Fr_{tp} = (16\ m^2/\pi^2 D^5 g)[X^2/\rho_v^2 + (1-X)^2/\rho_l^2] \qquad (9)$$

Comparing low-g and vertical downward terrestrial flow one has to correct the latter for the reduction of the slipfactor by the gravity forces assisting the downflowing liquid layer. Anyhow, vertical downflow is the preferred two-phase line orientation in the terrestrial model because of the axial-symmetric flow pattern. A similar conclusion can be drawn for the straight tube condenser. Recalling Fig. 1, it is remarked that in the condensers the flow will change from wavy annular mist to pure liquid flow passing several flow patterns, depending on the traject of the condensation.

QUANTITATIVE EXAMPLES - Consequences of scaling are elucidated by the Figs. 2 and 3, depicting the temperature dependence of the groups $g.Mo_l$ or $\rho_l\sigma^3/\mu_l^4$ and σ/ρ_l, a constituent of $(We/Fr)^{1/2}$.
Scaling at the same gravity level - First, it can be seen in Fig. 2 that the value $\rho_l\sigma^3/\mu_l^4 = 2*10^{12}\ m/s^2$ can be realised by seven systems: 115°C ammonia, 115°C methanol, 35°C water, 180°C propanol, 235°C propanol, 250°C thermex and 350°C thermex. Requiring, in addition to Morton Number identity, also the identity in $(We/Fr)^{1/2}$, in other words $D/(\sigma/\rho_l)^{1/2}$, the length scales of the seven systems derived from the corresponding (a/P,)-values in Fig. 3, turn out to be proportional to each other with ratios 2.5 : 4.5 : 8.4 : 4.2 : 3.0 : 5.0 : 3.6. Hence the maximum scaling ratio obtainable equals $8.4/2.5 \approx 3$, indicating that geometry scaling at the same gravity level can cover only a limited range.
Second, the scaling of high pressure (say 110 “C) ammonia system parts by low pressure (say -50 “C) ammonia system parts might be attractive for safety reasons or to reduce the impact of earth gravity in vertical two-phase sections. Similarly to the above, one can derive from Fig. 3 that the length scale ratio between the high-pressure prototype and low-pressure model (both characterised by
$\rho_l\sigma^3/\mu_l^4 = 2.10^{n}\ m/s^2$) is $L_p/L_m = [(\sigma/\rho_l)_p/\sigma/\rho_l)_m]^{1/2} \approx 0.4$.
For ammonia such a scaling can be attractive only for sections without heat transfer, since otherwise it will certainly lead to unacceptable high power levels in the model system evaporators and condensers.
Scaling with respect to gravity - Fig. 2 shows that the scaling with respect to gravity is restricted to say two decades, if the fluid in prototype and model is the same. For example a 10^{-2} g, 80 °C thermex prototype can be scaled by a 300 °C thermex model on earth. The length scaling is $L_p/L_m = D_p/D_m = (g_m/g_p)^{1/4}(\sigma/\rho_l)_p^{1/4}/(\sigma/\rho_l)_m^{1/4} \approx 14$.

Far more interesting is fluid to fluid scaling: e.g. alkali metal terrestrial prototypes can be scaled by various model systems in space, e.g. a 400°C mercury prototype:
- At 10^{-2} g, by a 35°C ammonia model ($L_m/L_p \approx 11$) or 80°C water model ($L_m/L_p \approx 14$).
- At 10’ g, by a methanol model at 35°C ($L_m/L_p \approx 95$), a 130°C thermex ($L_m/L_p \approx 100$) a or 30°C R114 ($L_m/L_p \approx 45$).

It is obvious that space-oriented mercury systems must be scaled on by other fluid systems in centrifuges on earth.
Finally it can be said that a 25°C R114 prototype at 10^{-2} g can be scaled by a 25°C 1 g ammonia model ($L_p/L_m \approx 5$)., important for the ESA developments discussed next.
Useful experiments- To support ESA two-phase activities (TPX I and TPHTS), experiments had to be carried out using the NLR two-phase test rig. This ammonia rig, having approx. the same line diameter as the TPX I loop, has been used for:
- The development, testing and calibration of TPX I&II components.
- The scaling of low-gravity adiabatic and condensing flow as discussed in the following sections: terrestrial low temperature vertical downflow minimises the impact of gravity, hence simulates low-gravity conditions the best.

In addition it is recalled that the the full size low-gravity ($<10^{-2}$ g) mechanically-pumped R114 ESA TPHTS can be adequately scaled by the above ammonia test rig, since:
- The, say 10^{-2} - 10^{-3} g, R114 prototype and the terrestrial ammonia model have approximately identical Morton numbers.
- This fluid to fluid scaling leads towards a corresponding length scaling $D_p/D_m = (g_m/g_p)^{1/2} \cdot (\sigma/\rho_l)^{1/2}_p/(\sigma/\rho_l)^{1/2}_m \approx$ 4.5 to 6.5, which is in agreement with the ratio of the actual diameters, being 21 mm for the R114 space-oriented prototype and 4.93 mm for the terrestrial ammonia model.

Concluding Remarks - The scaling of two-phase heat transport systems is very complicated. Only distorted scaling offers some possibilities, especially when not the entire loop but only loop sections are involved.
Scaling with respect to gravity is hardly discussed in literature. Some possibilities can be identified, for typical and very limited conditions only.
The mechanically pumped NLR two-phase ammonia test rig offers: Some opportunities to scale a TPX I ammonia loop and a very promising application: the terrestrial scaling of a ESA mechanically pumped TPHTS (R114) flight unit.

PREDICTIONS VERSUS EXPERIMENTAL RESULTS -
As stated before, an important quantity to be measured during two-phase flow experiments is the pressure drop in adiabatic sections and in condensers: sections considered crucial for two-phase system modelling and scaling. Therefore we will concentrate in the following on pressure drops in condensing and adabatic flow and restrict the discussion to straight tubes.

Modellina eauations - The total local (z-dependent) pressure gradient for annular two-phase flow is the sum of friction, momentum and gravity gradients:

$$dp(z)/dz)_t = (dp(z)/dz)_f + (dp(z)/dz)_m + (dp(z)/dz)_g. \quad (10)$$

Following Delil, 1991 & 1992, based on Soliman et al., 1968 (an elaborate publication on the subject), one can write for the contribution of friction (deleting the z-dependence to shorten the notation):

$$(dp/dz)_f = -(32\dot{m}^2/\pi^2\rho_v D^5)(0.045/Re_v^{0.2})[X^{1.8} + 5.7(\mu_l/\mu_v)^{0.0523}(1-X)^{0.47}X^{1.33}(\rho_v/\rho_l)^{0.261} + 8.1(\mu_l/\mu_v)^{0.105}(1-X)^{0.94}X^{0.86}(\rho_v/\rho_l)^{0.522}]. \quad (11)$$

X is the local quality X(z), Re, is the Reynolds number

$$Re, = 4\dot{m}/\pi D\mu_v \quad (12)$$

The fluid properties μ_l, μ_v, ρ_l and ρ_v are assumed to be independent of z, since they depend only on the mixture temperature, which usually is almost constant in adiabatic and condensing sections.

The momentum constituent can be written as

$$(dp/dz)_m = -(16\dot{m}^2/\pi^2D^4)\{[2X(1-\alpha)/\rho_v\alpha^2 - \beta(1-X)/\rho_l\alpha + (1-\beta)(1-X)/\rho_l(1-a) + (1-X)/\rho_l(1-\alpha)](dX/dz) + [X^2(1-\alpha)/\rho_v\alpha^3 + (1-X)^2/\rho_l(1-\alpha)^2](d\alpha/dz)\}. \quad (13)$$

α is the z-dependent local void fraction a(z). β = 2 for laminar liquid flow, β = 1.25 for turbulent flow.
The gravity constituent is

$$(dp/dz)_g = (1-\alpha)(\rho_l-\rho_v)g\cos\nu. \quad (14)$$

$g \rightarrow 0$ for microgravity conditions and g cosν equals 9.8 m/s^2 for vertical downflow on Earth, 3.74 m/s^2 for vertical downflow on Mars and 1.62 m/s^2 on the Moon.
α is eliminated in eq. (13) and eq. (14) by inserting eq. (1).

The slipfactor S is to be specified. The principle of minimum entropy production (Zivi, 1964) leads to.

$$s = [(1+1.5Z)(\rho_l/\rho_v)]^{1/3} \quad (15)$$

for annular flow, in which the constant Z (according to experiments) is above 1 and below 2.

$$S = \{(\rho_l/\rho_v)[1+Z'(\rho_v/\rho_l)(1-X)/X]/[1+Z'(1-X)/X]\}^{1/3} \quad (16)$$

for real annular-mist flow, that is annular flow with a mass fraction Z' of liquid droplets entrained in the vapour core. Z' is between 0 for zero entrainment and 1 for complete entrainment. For the limiting cases $Z \rightarrow 0$ and $Z' \rightarrow 0$, eqs. (15) and (16) become:

$$s = (P/P'')^{1/n} \quad (17)$$

The latter relation, representing ideal annular flow, will be used here for reasons of simplicity and since it allows a comparison with the results of calculations found in literature. The influence of $Z \neq 0$ and $Z' \neq 0$ is an interesting subject for future investigations.
Inserting eq. (17) into eq. (1) and eqs. (11, 13, 14), yields

$$(dp/dz)_m = -(32\dot{m}^2/\pi^2\rho_v D^5)(D/2)(dX/dz) \cdot [2(1-X)(\rho_v/\rho_l)^{2/3} + 2(2X-3+1/X)(\rho_v/\rho_l)^{4/3} + (2X-1-\beta X)(\rho_v/\rho_l)^{1/3} + (2\beta-\beta X-\beta/X)(\rho_v/\rho_l)^{5/3} + 2(1-X-\beta+\beta X)(\rho_v/\rho_l)]. \quad (18)$$

$$(dp/dz)_g = (32\dot{m}^2/\pi^2\rho_v D^5)\{1-[1+(\rho_v/\rho_l)^{2/3}(1-X)/X]^{-1}\} \cdot * [\pi^2 D^5 g\cos\nu(\rho_l-\rho_v)\rho_v/32\dot{m}^2]. \quad (19)$$

To solve eqs. (11, 18, 19) an extra relation is necessary, defining the z-dependence of X. A relation often used

$$dX/dz = -X_{entrance}/L_c \qquad (20)$$

(L_c being the condensation length), means uniform heat removal (hence a linear decrease of vapour quality along the duct), which may be unrealistic. It is better to use

$$-h_{lv}(dX/dz) = -h\pi D[T(z)-T_s] \qquad (21)$$

relating local quality and heat transfer. h represents the local heat transfer coefficient h(z), for which one can write

$$h = 0.01\ 8(k_l\rho_l^{1/2}/\mu_l)Pr_l^{0.65}|-(dp/dz)_f|^{1/2}D^{1/2} \qquad (22)$$

The latter equation has been derived (Soliman et al. 1968) assuming that the major thermal resistance exists in a laminar sublayer of the turbulent condensate film.
As already mentioned the two-phase flow traject is almost isothermal, which implies constant temperature drop T(z) - T_s (for constant sink temperature T_s), constant fluid properties and constant Prandtl number, defined by

$$Pr_l = Cp_l\ \mu_l\ /k_l. \qquad (23)$$

The total condensation pressure drop is

$$\Delta p_t = \int_0^{l-c} (dp/dz)_f dz. \qquad (24)$$

Eqs. (10, 11, 18, 19, 21) and eq. (22) can be combined, yielding an implicit non-linear differential equation in the variable X(z), which can be rewritten into a solvable standard form for differential/ algebraic equations

$$F(dX/dz, X) = 0. \qquad (25)$$

Adiabatic flow – Fig. 4, comparing the pressure gradient constituents at two temperatures, proves that the gravity constituent is overruled by the others at low temperature. This means that low-g behaviour can be investigated by terrestrial tests at low temperature. Calculations for adiabatic annular flow pressure gradients (Delil, 1991), according to the equations presented above, confirm (Fig. 5) the pressure drops over an adiabatic section determined experimentally during low-gravity aircraft flights with a R114 system (Chen et al., 1991).

Condensation lenaths - The modelling and calculations have been extended from adiabatic towards condensing flow in a straight condenser duct (Delil, 1992) to investigate the impact of gravity level on the duct length required to achieve complete condensation. This impact, which has been reported to lead to duct lengths up to more than one order of magnitude larger for zero gravity as compared to horizontal orientation in Earth gravity (Da Riva & Sanz, 1991), has been assessed (Delil, 1992) for various mass flow rates, duct diameters and thermal (loading) conditions, for two working fluids i.e. ammonia (working fluid for the Space Station, for capillary pumped two-phase systems and for TPX) and R114 (working fluid of the ESA TPHTS).

A summary of results of calculations carried out for ammonia, the most promising working fluid for future two-phase systems, is presented next.
To compare the results of the calculations with data from literature, the condenser defined by Da Riva & Sanz, 1991, was chosen as the baseline (main characteristics are power Cl = 1000 W, line diameter D = 16.1 mm, ammonia temperature T = 300 K and a temperature drop to sink ΔT = 10 K. The other parameter values are:

T	(K)	300	243	333
h_{lv}	(J/kg)	$1.16*10^6$	1.36'1 0^6	$1.00*10^6$
m	(kg/s)	8.64'1 0^{-4}	7.36'1 0^{-4}	9.98'10'
μ_l	(Pa.s)	$1.40*10^{-4}$	$2.47*10^{-4}$	0.94'10'
μ_l/μ_v	(-)	12.30	30.66	8.54
ρ_l	(kg/m^3)	6 0 0	678	545
ρ_l/ρ_v	(-)	72.46	652.4	26.6
k_l	(W/m.K)	0.465	0.582	0.394
Pr	(-)	1.42	1.90	1.25

Gravity levels considered are zero gravity g=0, Earth gravity (l-g) g=9.8 m/s^2, Mars gravity g=3.74 m/s^2, Moon gravity g=1.62 m/s^2, and 2-g macrogravity level 19.6 m/s^2. Illustrative results of calculations are discussed next.
Fig. 6 shows the vapour quality X along the condensation traject (as a function of non-dimensional condensation length z/D) for all gravity levels mentioned, including the curves of Da Riva & Sanz, 1991, for zero-g and horizontal condensation on earth. The curves start at entrance quality 0.96 for which annular flow, is expected to be established.
From this figure it can be concluded that:

- The length required for full condensation strongly increases with decreasing gravity: zero-gravity condensation length is roughly 10 times the terrestrial condensation length.
- The data presented by Da Riva & Sanz, 1991, can be considered as extremes: a horizontal condensation length of say 50% of the terrestrial downflow length (induced by the stratified flow pattern that enhances the transfer area and heat transfer coefficient) and higher zero-g predictions (induced by the equation for the heat transfer coefficient used, being different from the model presented here).

To assess the impact of the fluid saturation temperature on condensation performance, similar curves have been calculated for two other temperatures, 243 K and 333 K and the parameter values given above (Delil, 1992).
The calculations show that the full condensation length increases with the temperature for zero gravity conditions, but decreases with temperature for the other gravity levels. This implies that the differences between Earth gravity and low-g outcomes decrease with decreasing temperature, confirming the statement already made: the effect of gravity is reduced in low temperature vertical downflow.
Calculations of the vapour quality distribution along the 16.1 mm reference duct for condensing ammonia (at 300 K) under Earth gravity and O-g conditions, for power levels ranging from 0.5 kW up to 25 kW, yielded (Delil, 1992) that:

- A factor 50 in power, 25 kW down to 500 W, corresponds in a zero gravity environment to a relatively minor

reduction in full condensation length, i.e. from say 600 D to 400 D (from 9.5 to 6.5 m).
- Under Earth gravity conditions, power and full condensation length are strongly interrelated: from L_c = 554 D at 25 kW to only 19 D at 500 W.
- The gravity dependene of the full condensation length decreases with increasing power, until the differences vanish at roughly 1 MW condenser choking conditions. The latter value is an upper limit, calculated (following Zivi, 1964) for ideal annular flow. Choking may occur at considerably lower power values in the case of actual annular-wavy-mist flow, but the value exceeds anyhow the homogeneous flow choking limit, roughly 170 kW.

Calculation of the vapour quality along the duct for three gravity levels (0, Earth and 2-g) and three duct diameters (8.05, 16.1 and 24.15 mm) at 300 K, yielded the ratio of the absolute duct lengths L_c(m) needed for full condensation under zero-g and one-g respectively (Delil, 1992). It has been concluded that the ratio between full condensation lengths in zero-g and on Earth ranges from roughly 1.5 for the 8.05 mm duct, via 11 for the 16.1 mm duct, up to more than 30 for the 24.15 mm duct. In other words, smaller line diameter systems are less sensitive for differences in gravity levels as compared with larger diameter systems. The above is confirmed by TPX I flight data (Delil, 1995).

Since the model developed is valid for pure annular flow only, it is worthwhile to investigate the impact of other flow patterns present inside the condenser duct (mist flow at the high quality side, slug and bubbly flow at the low quality side and wavy-annular-mist in between), in other words to investigate whether the pure annular flow assumption, leads towards slightly or substantially overestimated full condensation lengths. A further complication is the lower boundary of the annular-wavy-mist flow pattern. In addition, flow pattern transitions occur at vapour quality values, that strongly depend on temperature and line diameter.

Summary - The information presented confirms the results of other models i.e. when designing condensers for space applications, one should carefully use and interpret data obtained from terrestrial condenser tests, even when the latter pertain to vertical downward flow situations (characterised by the same flow pattern).
The model equations given are useful for a better understanding of the problems that can be expected: problems related to flow and heat transfer (necessary lengths of condensers for space applications).
The equations and the results of the calculations suggest that hybrid scaling exercises, which combine geometrical and fluid-to-fluid scaling, can beneficently support the design of space-oriented two-phase heat transport systems and their components.
With respect to the local heat transfer equation used, eq. (22), it can be remarked that it has a wrong lower limit $h \to 0$ for $(dp/dz)_f \to 0$, which disappears by incorporating conduction through the liquid layer. Preliminary calculations indicate that the incorporation of pure conduction will lead to somewhat shorter full condensation lengths, both for zero-g and for non-zero-g conditions. This implies quantitative changes only, in other words the conclusions presented above remain valid.

FLOW PATTERN ASPECTS - Accurate knowledge of the gravity level dependent two-phase flow regimes is crucial for modelling and designing two-phase heat transport systems for space, as flow patterns directly affect thermal hydraulic characteristics of two-phase flow and heat transfer. Therefore flow pattern maps are to be created, preferably in the non-dimensional format of Fig. 1.

Hamme & Best, 1997, created, based on many low-gravity aircraft flight data (with a R12, 10.5 mm lines experiment), three dimensional flow pattern maps shown in Fig. 7. Fig. 8 summarises their O-g data. Fig. 9 shows the O-g map, derived from TPX I (ammonia, 5.3 mm lines) VQS flight data. Fig. 10 depicts data of recent low-g aircraft experiments with Cyrène, an amonia system with a 4.7 mm line diameter (Lebaigue et al., 1996).
A comparison between the Figs. 8 to 10 suggests that the transition to annular flow occurs in these three systems at the same j_v-value 0.25-0.3 m/s, but at j_l-values that depend on line size or working fluid.
It is clear that a lot of work has to be done before such maps are mature, preferably in the format of Fig. 1.

NOMENCLATURE

A	area	m^2
Bo	boiling number	
CP	specific heat at constant pressure	J/kgK
D	diameter	m
d	diameter of curvature	m
Eu	Euler number	
Fr	Froude number	
g	gravitational acceleration	m/s^2
H	enthalpy	J/kg
h	heat transfer coefficient	W/m^2K
h_{lv}	latent heat of vaporisation	J/kg
j	superficial velocity	m/s
k	thermal conductivity	W/mK
L	length	m
Ma	Mach number	
Mo	Morton number	
$\dot{m}$	mass flow rate	kg/s
Nu	Nusselt number	
p	pressure	N/m^2
Pr	Prandtl number	
Q	power	W
q	heat flux	W/m*
Re	Reynolds number	
S	slip factor	
T	temperature	K
t	time	s
v	velocity	m/s
We	Weber number	
X	vapour quality	
z	axial or vertical coordinate	m
α	vapour fraction (volumetric)	
β	constant in eq. (13)	

δ	surface roughness	m
A	difference, drop	
μ	viscosity	Ns/m^2
σ	surface tension	N/m
Π	dimensionless number	
ρ	density	kg/m^3
v	angle (with respect to gravity)	rad

Subscripts

a	acceleration	p	pore, prototype
c	condenser	s	entropy
f	friction	t	total
g	gravitation	tp	two-phase
l, ℓ	liquid	v	vapour
m	momentum, model	w	water
o	reference condition		

REFERENCES

Amadieu, M. et al., 1997, Development of a Deployable Radiator using a LHP as Heat Transfer Element, Proc. 6th European Symp. on Space Environmental Control Systems, Noordwijk, Netherlands, ESA SP-400, 283-288.

Antoniuk, D. & Nienberg, J., 1998, Analysis of Salient Events in the Two-Phase Thermal Control Flight Experiment, SAE 981817, 28th Int. Conf. on Environmental Systems, Danvers, USA.

Baker, C.L. & Bienert, W.B. & Ducao, A.S. ,1998, Loop Heat Pipe Flight Experiment, SAE 981580, 28th Int. Conf. on Environmental Systems, Danvers, USA.

Bienert, W.B. & Wolf, D.A., 1995, Temperature Control with Loop Heat Pipes: Analytical Model and Test Results, Proc. 9th Int. Heat Pipe Conf. Albuquerque, USA, 981-988.

Butler, D. & Ottenstein, L. & Ku, J., 1995, Flight Testing of the Capillary Pumped Loop Flight Experiments, SAE 951566, 25th Int. Conf. on Environmental Systems, San Diego, USA.

Chen, I. et al., 1991, Measurements and Correlation of Two-Phase Pressure Drop under Microgravity Conditions, J. of Thermophysics, 5, 514-523.

Cullimore, B., 1993, Capillary Pumped Loop Application Guide, SAE 932156, 23rd Int. Conf. on Environmental Systems, Colorado Springs, USA.

Cullimore, B. & Nikitkin, M., 1997, CPL and LHP Technologies: What are the Differences, What are the Similarities?, SAE 981587, 28th Int. Conf. on Environmental Systems, Danvers, USA.

Da Riva, I. & Sanz. A., 1991, Condensation in Ducts, Microgravity Science and Technology, 4, 179-l 87.

Delil, A.A.M., 1988, A Sensor for High-Quality Two-Phase Flow, NLR MP 88025 U, Proc. 16th Int. symp. on Space Technology and Science, Sapporo, Japan, 957-966.

Delil, A.A.M., 1991, Thermal Gravitational Modelling and Scaling of Two-Phase Heat Transport Systems: Similarity Considerations and Useful Equations, Predictions Versus Experimental Results, NLR TP 91477 U, European Symp. Fluids in Space, Ajaccio, France, ESA SP-353, 579-599.

Delil, A.A.M., 1992, Gravity Dependence of Pressure Drop and Heat transfer in straight two-phase heat transport system Condenser Ducts, NLR TP 92167 U, SAE 921168, 22nd Int. Conf. on Environmental Systems, Seattle, USA.

Delil, A.A.M., 1994, Two-Phase Flow and Heat Transfer in Various Gravity Environments, NLR TP 94407 U, 4th Int. Heat Pipe Symp., Tsukuba, Japan.

Delil, A.A.M. et al., 1995, TPX for In-Orbit Demonstration of Two-Phase Heat Transport Technology - Evaluation of Flight & Postflight Experiment Results, NLR TP 95192 U, SAE 95150, 25th Int. Conf. on Environmental Systems, San Diego, USA.

Delil, A.A.M., Dubois, M., Supper, W., 1997, The European Two-Phase Experiments: TPX I & TPX II, NLR TP 97502 U, 10th Int. Heat Pipe Conf., Stuttgart, Germany.

Delil, A.A.M., et al., 1998, Sensors and Components for Aerospace Thermal Control, Life Science and Propellant Systems, NLR TP 97504 U, AIP Conf. Proc. 420, Space Technology & Applications Int. Forum, Albuquerque, USA 514-521.

Dunbar, N.W., 1996, ATLID Laser Head Thermal Control-Design and Development of a Two-Phase Heat Transport System for Practical Application, SAE 961561, 26th Int. Conf. on Environmental Systems, Monterey, USA.

Geraets, J.J.M., 1986, Centrifugal scaling of isothermal gas-liquid flow in horizontal tubes, Thesis Technological University Delft.

Hagood, R., 1998, CCPL Flight Experiment: Concepts through Integration, SAE 981694, 28th Int. Conf. on Environmental Systems, Danvers, USA.

Hamme, T.A. & Best, F.R., 1997, Gravity Dependent Flow Regime Mapping, AIP Conf. Proc. 387, Space Technology & Applications Int. Forum, Albuquerque, USA, 635-640.

Kim, J.H., et al., 1997, The Capillary Pumped Loop III Flight Demonstration, Description, and Status, AIP Conf. Proc. 387, Space Technology & Applications Int. Forum, Albuquerque, USA, 623-628.

Ku, J. & Ottenstein, L. & Butler, D., 1996, Performance of CAPL 2 Flight Experiment, SAE 961431, 26th Int. Conf. on Environmental Systems, Monterey, USA.

Ku, J. & Yun, S, & Ottenstein, L, 1998, Design and test Results of CAPL-3 Engineering Test Bed and Ground Test

of CAPL-3 Flight Experiment, SAE 981812, 28th Int. Conf. on Environmental Systems, Danvers, USA.

Lebaigue, 0. & Bouzou, N. & Colin, C. , Cyrene: An Experimental Two-Phase Ammonia Fluid Loop in Microgravity. Results of a Parabolic Flight Campaign, SAE 981689, 28th Int. Conf. on Environmental Systems, Danvers, USA.

Maidanik, Y.F. & Solodovnik, N. & Fershtater, Y.G., 1995, Investigation of Dynamic and Stationary Characteristics of Loop Heat Pipe, Proc. 9th Int. Heat Pipe Conf. Albuquerque, USA, 1002-I 006.

Maidanik, Y.F. & Fershtater, Y.G. & Goncharov, K.A., 1991, Capilary Pump Loop for Systems of Thermal Regulation of Spacecraft, Proc. 4th European Symp. on Space Environmental Control Systems, Florence, Italy, ESA SP-324, 87-92.

Miller-Hurlbert, K., 1997, The Two-Phase Extended Evaluation in Microgravity Flight Experiment: Description and Overview, AIP Conf. Proc. 387, Space Technology & Applications Int. Forum, Albuquerque, USA, 547-554.

Orlov, A.A., et al., 1997, The Loop Heat Pipe Experiment Onboard the Granat Spacecraft, 6th European Symp. on Space Environmental Control Systems, Noordwijk, Netherlands., ESA SP-400, 341-353.

Oshinowo, T. & Charles, M.E., 1974, Vertical Two-Phase Flow, Flow Pattern Correlations, Can. J. Chem. Engng. 52, 25-35.

Ottenstein, L. & Nienberg, J., 1998, Flight Testing of the Two-Phase Flow Flight Experiment, SAE 981816, 28th Int. Conf. on Environmental Systems, Danvers, USA.

Soliman, M. & Schuster, J.R. & Berenson, P.J., 1968, A General Heat Transfer Correlation for Annular Flow Condensation, Trans. ASME, J. Heat Transfer, 90, 267-276.

Stenger, F.J., 1966, Experimental Study of Water-Filled Capillary Pumped Heat Transfer Loops, NASA X-l 310.

Zivi, S.M., 1964, Estimation of Steady-State Void Fraction by Means of the Principle of Minimum Entropy Production, Trans. ASME C, J. Heat Transfer, 86, 247-252.

Table 1 Relevance of π-numbers for thermal gravitational scaling of two-phase loops	Liquid Parts		Evaporators swirl & capillary	Non-liquid Lines vapour/2-phase	Condensers
	adiabatic	heating cooling			
π_1 = D/L = geometry	·	·	·	·	·
$\pi_2 = Re_\ell = (\rho v D/\mu)_\ell =$ inertia/viscous	·	·	·	·	·
$\pi_3 = Fr_\ell = (v^2/gD)_\ell$ = inertia/gravity	·	·	·	/•	·
$\pi_4 = Eu_\ell = (\Delta p/\rho v^2)_\ell$ = pressure head/inertia	·	·	·	·	·
π_5 = cos v = orientation with respect to g	·	·	·	/•	·
$\pi_6 = S =$ slipfactor = v_v/v_ℓ			·	·	·
π_7 = density ratio = ρ_v/ρ_ℓ			·	·	·
π_8 = viscosity ratio = μ_v/μ_ℓ			·	·	·
$\pi_9 = We_\ell = (\rho v^2 D/\sigma)_\ell$ = inertia/surface tension			·	/•	·
$\pi_{10} = Pr_\ell = (\mu Cp/k)_\ell$		·	·		·
$\pi_{11} = Nu_\ell = (hD/k)_\ell =$ convective/conductive		·	·		·
$\pi_{12} = k_v/k_\ell$ = thermal conductivity ratio			·		·
$\pi_{13} = Cp_v/Cp_\ell$ = specific heat ratio			·		·
$\pi_{14} = \Delta H/h_{\ell v}$ = enthalpy number = X = quality		·	·	·	·
$\pi_{15} = Mo_\ell = (\rho_\ell \sigma^3/\mu_\ell^4 g)$ = capillarity/buoyancy			·	/•	·
$\pi_{16} = Ma = v/(\partial p/\partial \rho)_s^{1/2}$			·	·	·
$\pi_{17} = (h/k_\ell)(\mu_\ell^2 g)^{1/3}$			·		·
$\pi_{18} = L^3 \rho_\ell^2 g\, h_{\ell v}/k_\ell \mu_\ell (T-T_o)$			·		·

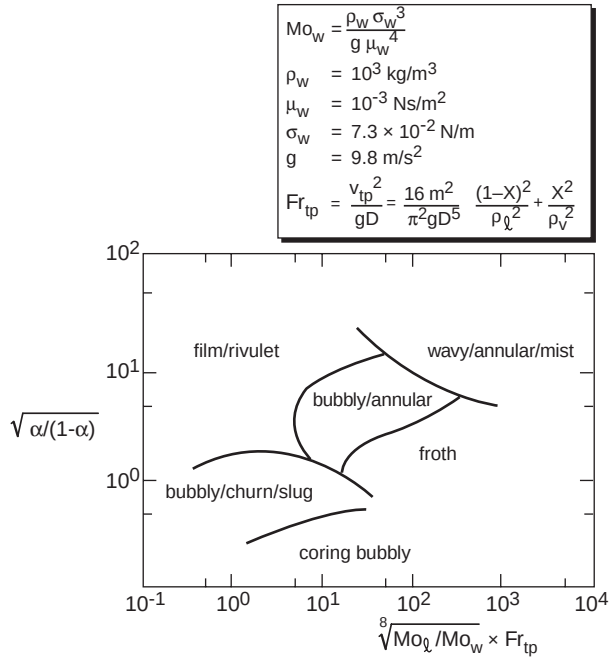

Fig. 1 Flow Pattern Map for Vertical Downward Flow

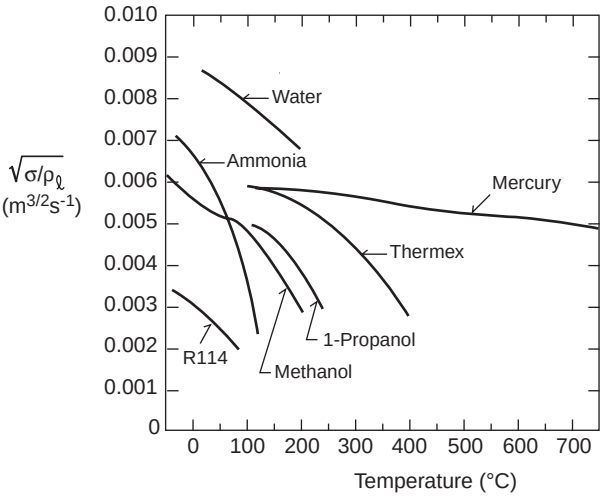

Fig. 3 $\sqrt{\sigma/\rho_\ell}$ versus Temperature for Various Fluids

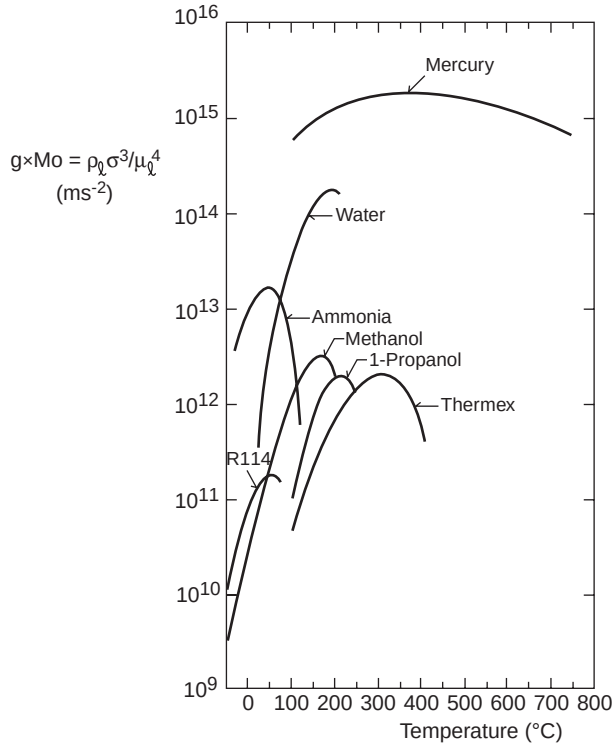

Fig. 2 The Grouping $\rho_\ell \sigma^3/\mu_\ell^4$ for Various Fluids, as a Function of the Temperature

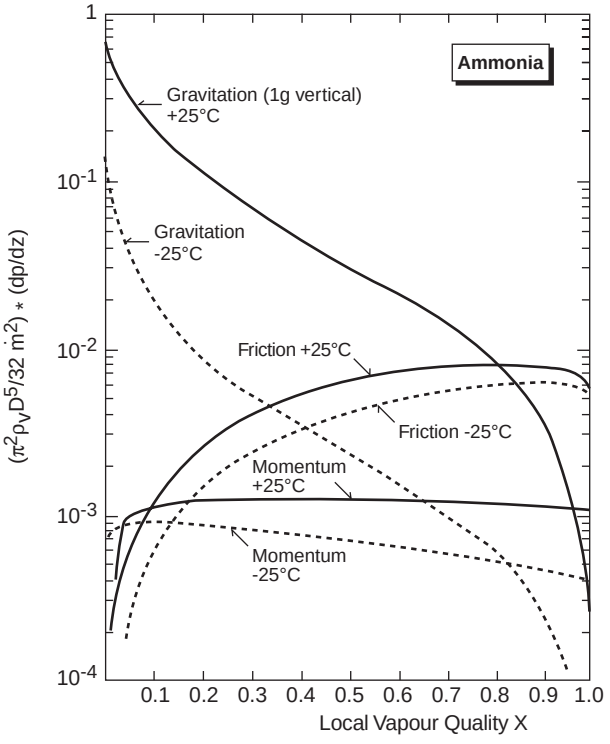

Fig. 4 Friction, Momentum and Gravity Contributions to the Local Pressure Gradient as a Function of the Vapour Quality

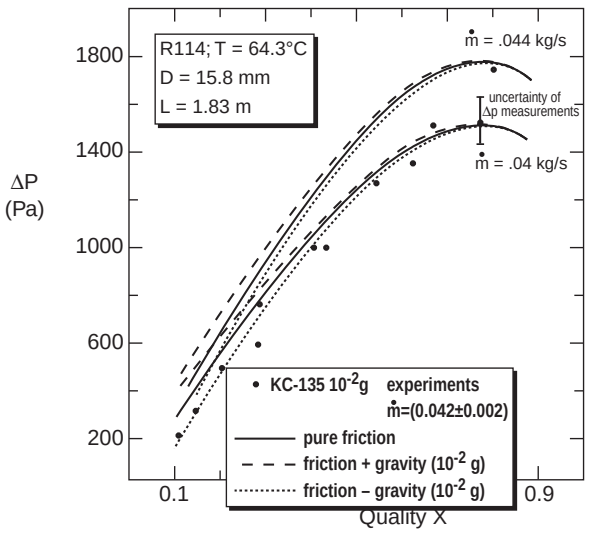

Fig. 5 Comparison of Measured and Predicted Adiabatic Pressure Drops for a R114 Duct

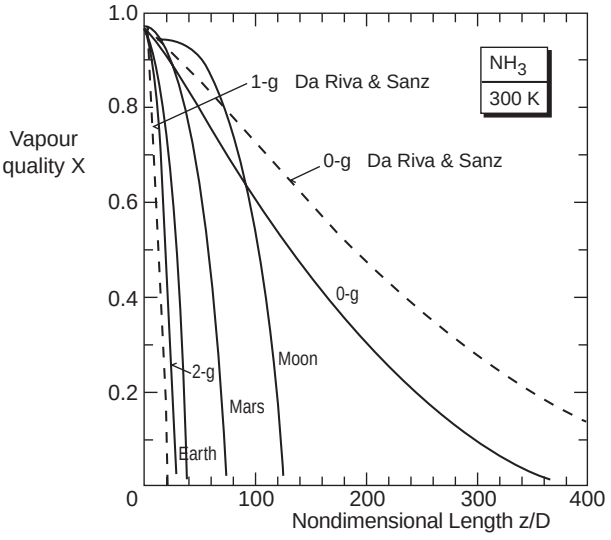

Fig. 6 Vapour Quality along the 16.1 mm Duct for Ammonia at 300 K (1000 W, ΔT = 10 K), for All Gravity Levels

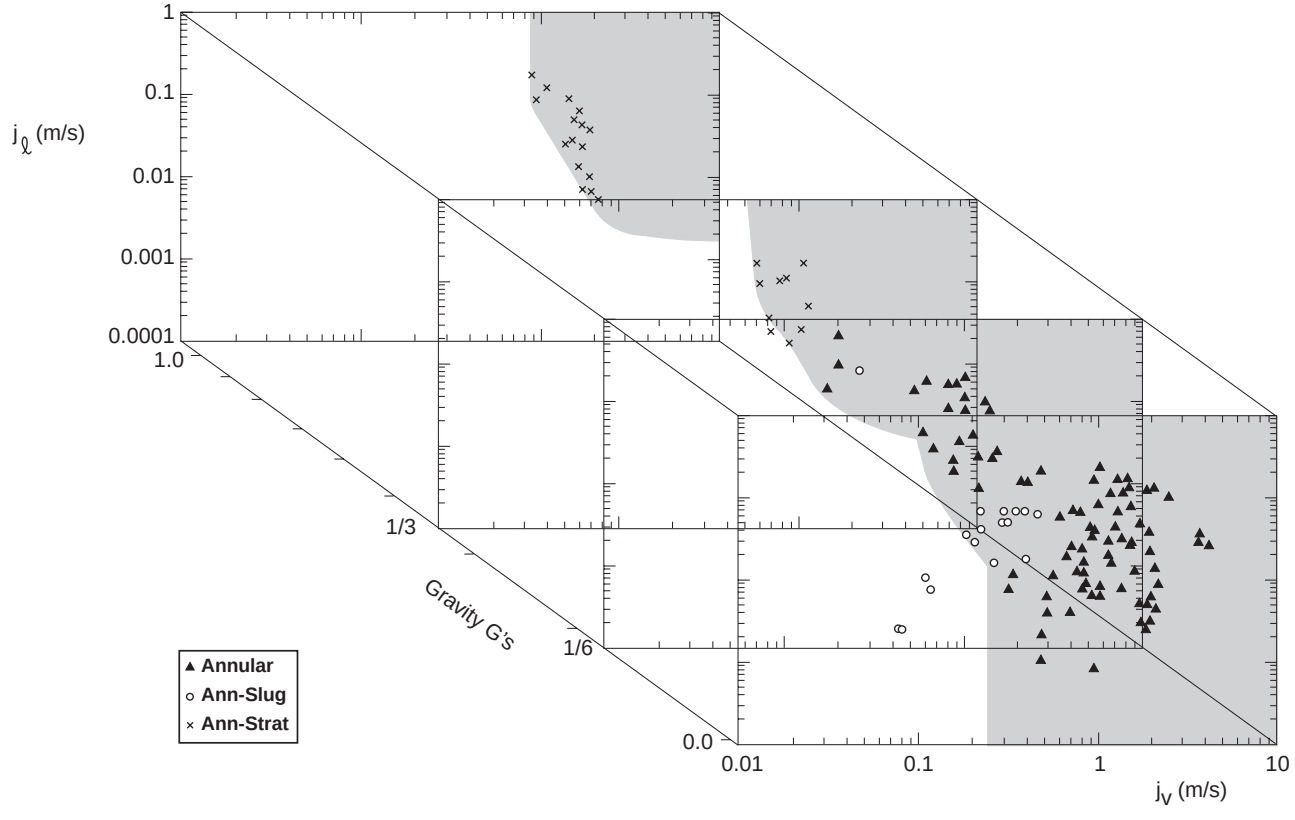

Fig. 7 3-D Flow Regime as a Function of Gravity Dependent Annular Flow Map

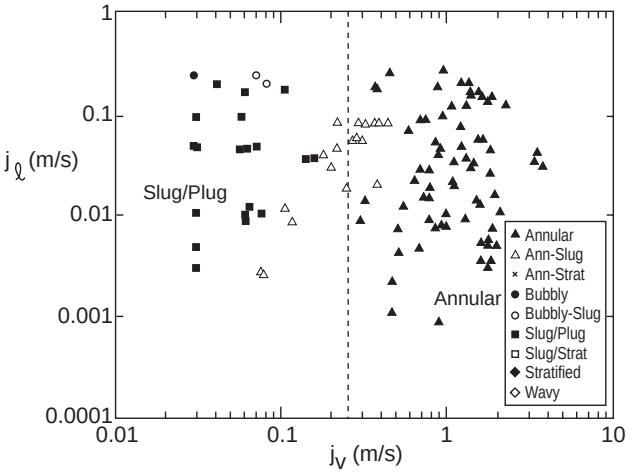

Fig. 8 Flow Regime Map in Microgravity (~0 G)

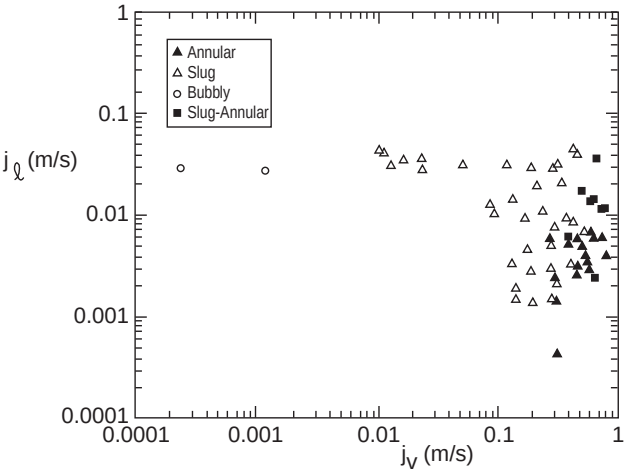

Fig. 10 Cyrène Flow Pattern Map

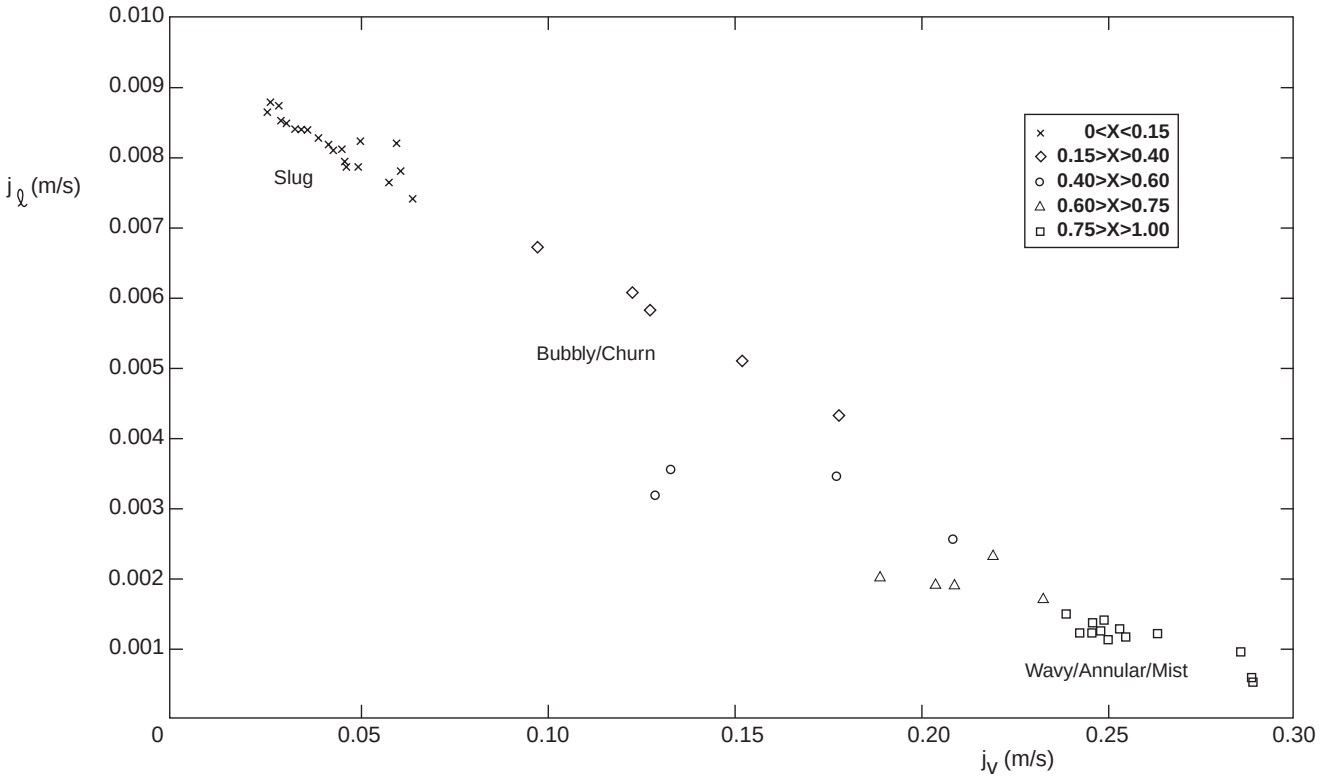

Fig. 9 Flow Patterns Derived from TPX I VQS Flight Data